

## Subsection B

### Assays of RGS Box Activity and Allosteric Control

#### [4] Fluorescence-Based Assays for RGS Box Function

By FRANCIS S. WILLARD, RANDALL J. KIMPLE, ADAM J. KIMPLE,  
CHRISTOPHER A. JOHNSTON, and DAVID P. SIDEROVSKI

#### Abstract

Ligand-activated, seven transmembrane-spanning receptors interact with inactive G-protein heterotrimers ( $G\alpha\beta\gamma$ ) to catalyze GTP loading and, consequently, activation of  $G\alpha$  subunits and the liberation of  $G\beta\gamma$ .  $G\alpha$ -GTP and  $G\beta\gamma$  are then competent to regulate independent effector pathways. The duration of heterotrimeric G-protein signaling is determined by the lifetime of the  $G\alpha$  subunit in the GTP-bound state. Signal termination is facilitated by the intrinsic guanosine triphosphatase (GTPase) activity of  $G\alpha$  and subsequent reformation of the inactive heterotrimer. Regulators of G-protein signaling (RGS) proteins act enzymatically, via their hallmark "RGS box," as GTPase-accelerating proteins (GAPs) for  $G\alpha$  subunits and thus function as negative regulators of G-protein signaling *in vitro* and *in vivo*. This article describes the use of fluorescence resonance energy transfer (FRET) to monitor the interaction between a  $G\alpha$  subunit and an RGS box protein. Furthermore, this article describes optimization of this assay for high-throughput screening and the evaluation of mutant RGS box and  $G\alpha$  proteins. Finally, this article describes the novel application of this FRET technique to measure the activity of RGS protein-derived GoLoco peptides that modulate  $G\alpha$  activation by aluminum tetrafluoride.

#### Introduction

Seven transmembrane-spanning receptors couple to second messenger pathways via heterotrimeric, guanine nucleotide-binding proteins (G proteins), which are composed of three subunits termed  $G\alpha$ ,  $G\beta$ , and  $G\gamma$  (Gilman, 1987; Pierce *et al.*, 2002). The  $G\alpha$  subunit is a molecular switch that is conformationally sensitive to guanine nucleotides. GDP-bound  $G\alpha$

is inactive and tightly associated with  $G\beta\gamma$ . Activated receptors catalyze guanine nucleotide exchange on the GDP-bound heterotrimer. GTP binding to  $G\alpha$  is thought to cause subunit dissociation and the activation of second messenger pathways by both  $G\alpha$ -GTP and  $G\beta\gamma$ . Signal termination is facilitated by the intrinsic guanosine triphosphatase (GTPase) activity of  $G\alpha$ . Thus, the duration of heterotrimeric G-protein signaling is determined by the lifetime of the  $G\alpha$  subunit in the GTP-bound state.

Regulator of G-protein signaling (RGS) proteins, characterized by their hallmark, ~120 amino acid “RGS box,” are GTPase-accelerating proteins (GAPs) for  $G\alpha$  subunits and thus act as negative regulators of G-protein signaling *in vitro* and *in vivo* (Neubig and Siderovski, 2002). Given their dynamic spatiotemporal regulation and receptor selectivity, RGS proteins represent promising targets for developing new therapeutic interventions (Neubig and Siderovski, 2002). *In vitro* measurements of RGS box GAP activity generally encompass radiolabeled guanine nucleotide hydrolysis assays (Berman *et al.*, 1996a), coprecipitation assays (Druey and Kehrl, 1997), or surface plasmon resonance (Kimple *et al.*, 2001; Popov *et al.*, 1997; see also this volume, Willard and Siderovski, 2004). Measurement of the RGS box-catalyzed nucleotide cycle has also been performed using both  $G\alpha$ -subunit intrinsic fluorescence (Lan *et al.*, 2000) and quench flow kinetic methods (Mukhopadhyay and Ross, 1999). This article describes methods for the use of fluorescence resonance energy transfer (FRET) to monitor the archetypal  $G\alpha$ /RGS box pair, namely the  $G\alpha_{i1}$ /RGS4 interaction (Tesmer *et al.*, 1997), both kinetically and at end point using a high-throughput methodology. Finally, we examine the application of this FRET technique to assay GoLoco peptides derived from RGS proteins that inhibit  $G\alpha_{i1}$  activation.

## Materials

Unless otherwise specified, all chemicals are of the highest purity obtainable from Sigma (St. Louis, MO) or Fisher Scientific (Pittsburgh, PA).

## Fluorescence Resonance Energy Transfer Assay

### Design Considerations

Fluorescence resonance energy transfer is the nonradiative transfer of energy from a donor fluorophore to an acceptor fluorophore. For a comprehensive discussion of the physical principles and practicalities of FRET, the reader is directed to the excellent resources of dos Remedios and Lakowicz (1999) and Moens (1995). Essentially, according to the Förster equation, FRET will be determined by (1) donor fluorophore

quantum yield, (2) donor/acceptor spectral overlap, (3) physical distance between donor and acceptor, and (4) orientation of the acceptor adsorption and donor emission dipoles. Derivatives of the enhanced *Aequorea victoria* green fluorescent protein (Prasher *et al.*, 1992), cyan fluorescent protein (ECFP) and yellow-fluorescent protein (EYFP), have been optimized for FRET given the wide spectral shift between the excitation wavelength required for ECFP and the emission wavelength of excited EYFP (Miyawaki and Tsien, 2000). At the present time, ECFP and EYFP, hereafter referred to as CFP and YFP, are the premium choice for genetically encoded acceptor and donor fluorophores, respectively.

To complement *in silico* computational approaches (Willard *et al.*, 2004) and facilitate high-throughput screening for small molecule inhibitors of RGS box/ $G\alpha$  interactions, we have developed a homogeneous FRET-based assay for the protein-protein interaction between RGS4 and  $G\alpha_{i1}$  (Kimple *et al.*, 2003). This assay uses the exquisite sensitivity of RGS4 for transition-state ( $GDP\cdot AlF_4^-$ )  $G\alpha_{i1}$  versus inactivated ( $GDP$ ) or pseudo-activated ( $GTP\gamma S$ ) state  $G\alpha_{i1}$  (Berman *et al.*, 1996b). In theory, fusion of CFP to  $G\alpha_{i1}$  and fusion of YFP to RGS4 provides a FRET pair that responds to aluminum tetrafluoride-induced activation of  $G\alpha_{i1}$  by an attenuated emission of the CFP donor and increased emission of the YFP acceptor, as outlined in Fig. 1A.

#### Cloning and Purification of $G\alpha_{i1}$ -CFP and YFP-RGS4

To create an expression construct for the YFP-RGS4 fusion protein, the citrine mutant of YFP [amino acids 1–237 of the pEYFP-C1 open reading frame (ORF); BD Biosciences Clontech, Palo Alto, CA] with a Q69M mutation (Heikal *et al.*, 2000) and the entire ORF of mouse RGS4 (amino acids 1–205; SwissProt RGS4\_MOUSE) were cloned in-frame with the N-terminal hexahistidine tag ( $His_6$ ) and tobacco-etch virus (TEV) protease cleavage site of the prokaryotic expression vector pProEXHTb (Invitrogen, Carlsbad, CA) using polymerase chain reaction and standard molecular biology techniques. In a similar fashion, the ORF of human  $G\alpha_{i1}$  (amino acids 1–353; SwissProt GBI1\_HUMAN) and the ORF of CFP (amino acids 1–239 of the pECFP-C1 ORF; BD Biosciences Clontech) were cloned in-frame with the  $His_6$ /TEV site of pProEXHTc to create the expression construct for the  $G\alpha_{i1}$ -CFP fusion protein.

Proteins were purified following overexpression in *Escherichia coli* using standard chromatographic procedures (Kimple *et al.*, 2001; see also this volume, Willard and Siderovski, 2004). Briefly, both  $G\alpha_{i1}$ -CFP and YFP-RGS4 fusion proteins were purified by the sequential application of  $Ni^{2+}$  affinity chromatography (HiTrap chelating HP; Amersham

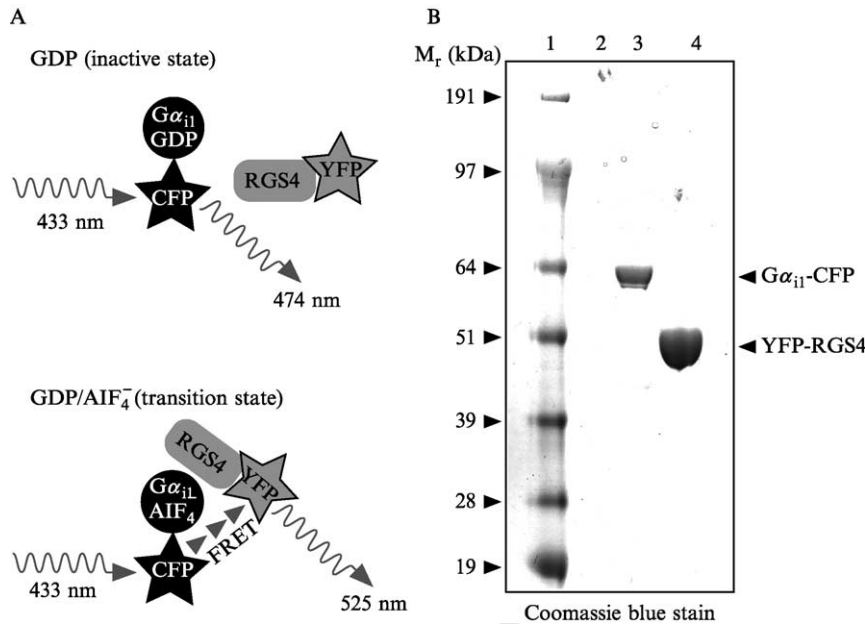


FIG. 1. (A) Schematic of fluorescence resonance energy transfer (FRET) assay for the  $G\alpha_{i1}$ -RGS4 interaction. In solution,  $G\alpha_{i1}$ -GDP-CFP does not interact with YFP-RGS4 and thus excitation of CFP at 433 nm results in high donor fluorophore emission at 474 nm. Transition-state  $G\alpha_{i1}$ -GDP·AlF $_4^-$ -CFP interacts with YFP-RGS4, bringing the CFP and YFP moieties into close proximity (<100 Å). Consequently, excitation energy of the donor fluorophore (CFP) is transferred to the acceptor fluorophore (YFP) and results in increased acceptor emission at 525 nm but reduced donor emission at 474 nm. (B) Electrophoretic analysis of purified  $G\alpha_{i1}$ -CFP and YFP-RGS4. Purified protein samples were resolved using 4–12% (w/v) SDS–polyacrylamide gel electrophoresis and Coomassie Blue staining. Lane 1, See Blue Plus 2 molecular weight standards (Invitrogen); lane 2, blank; lane 3, purified  $G\alpha_{i1}$ -CFP fusion protein; and lane 4, purified YFP-RGS4 fusion protein. Positions of molecular weight standards,  $G\alpha_{i1}$ -CFP, and YFP-RGS4 are denoted with arrowheads.

Bioscience, Uppsala, Sweden), anion-exchange chromatography (Source 15Q; Amersham), and gel-exclusion chromatography (HiPrep 26/60 Sephacryl S200 HR; Amersham). Figure 1B illustrates representative purifications of the His $_6$ - $G\alpha_{i1}$ -CFP and His $_6$ -YFP-RGS4 fusion proteins, respectively. The predicted molecular masses and molar extinction coefficients (at 280 nm) are 71.5 kDa and 63,400  $M^{-1}cm^{-1}$  for His $_6$ - $G\alpha_{i1}$ -CFP and 53.5 kDa and 43,060  $M^{-1}cm^{-1}$  for YFP-RGS4. Protein quantitation is performed by denaturation with 8 M guanidine HCl (Sigma) and absorption measurements at 280 nm (see in this volume, Willard and Siderovski, 2004) to obviate any effects of fluorescence from the CFP or YFP moieties on other protein assay methodologies.

### FRET-Based Assay of RGS4/ $G\alpha_{i1}$ Interaction

Measurements of CFP and YFP fluorescence are made in a LS55 luminescence spectrofluorimeter (Perkin Elmer, Boston, MA). The LS55 cuvette holder is water jacketed and thus can be connected to a circulating water bath to provide controlled temperature between 4 and 40°. Proteins are incubated in 2-ml quartz cuvettes (Fisher) with magnetic stirring bars (Fisher) containing 1 ml of buffer F (10 mM Tris-HCl, pH 8.0, 1 mM EDTA, 50 mM NaCl, 10 mM  $MgCl_2$ , 2  $\mu M$  GDP). The water bath temperature is set to 20°, and magnetic stir bars are rotated using the interactive command menus in the LS55 control program “FL WinLab” (Perkin Elmer) and selecting STATUS, SAMPLER ACCESSORY, CELL CHANGER STIRRER HIGH. We have found the inclusion of low concentrations of NaCl to be essential for the long-term stability of protein complexes during FRET measurements.  $MgCl_2$  and GDP are included in all solutions as they participate in the formation of the  $AlF_4^-$ -induced  $G\alpha$  transition state and their presence in all cuvettes obviates any background fluorescence changes due to these compounds.

Excitation and emission maxima for CFP, YFP, and FRET complexes can be determined using the SCAN utility and selecting PRESCAN, which provides a rapid evaluation of both excitation and emission spectra. Subsequently, the EMISSION and EXCITATION SCAN utilities can be used to obtain spectral data more accurately. Based on such analysis, the optimal conditions for detecting CFP/YFP FRET can be determined. To this end, CFP fluorescence is excited at 433 nm and sequential emission scans are recorded at 0.5-nm intervals between 450 and 600 nm, at a speed of 50 nm/min, with excitation and emission slit widths of 2.5 nm. Excitation and emission spectra are analyzed using Graph Pad Prism version 4.0 (Graph Pad Software, San Diego, CA). Spectra are corrected for buffer absorption by subtracting the values of a cuvette containing only buffer; data can then be expressed in relative fluorescence units and are scaled to give one specific spectrum, namely the YFP-RGS4 alone spectrum, a maximal emission of 100 (e.g., Fig. 2A).

The fluorescence emission spectrum ( $\lambda_{ex} = 433$  nm) of 1  $\mu M$   $G\alpha_{i1}$ -CFP is illustrated in Fig. 2A.  $G\alpha_{i1}$ -CFP has an emission maximum at 474 nm within a broad spectrum characterized by a “shoulder” extending to a second inflexion point at 500 nm. One micromolar YFP-RGS4 has an emission maximum at 525 nm (Fig. 2A); however, at  $\lambda_{ex} = 433$  nm, the relative intensity of YFP emission is low (as the excitation maximum of YFP is 516 nm). The fluorescence emission spectrum ( $\lambda_{ex} = 433$  nm) of 1  $\mu M$   $G\alpha_{i1}$ -CFP and 1  $\mu M$  YFP-RGS4 in the same cuvette is simply the sum of the individual  $G\alpha_{i1}$ -CFP and YFP-RGS4 spectra (Fig. 2A).

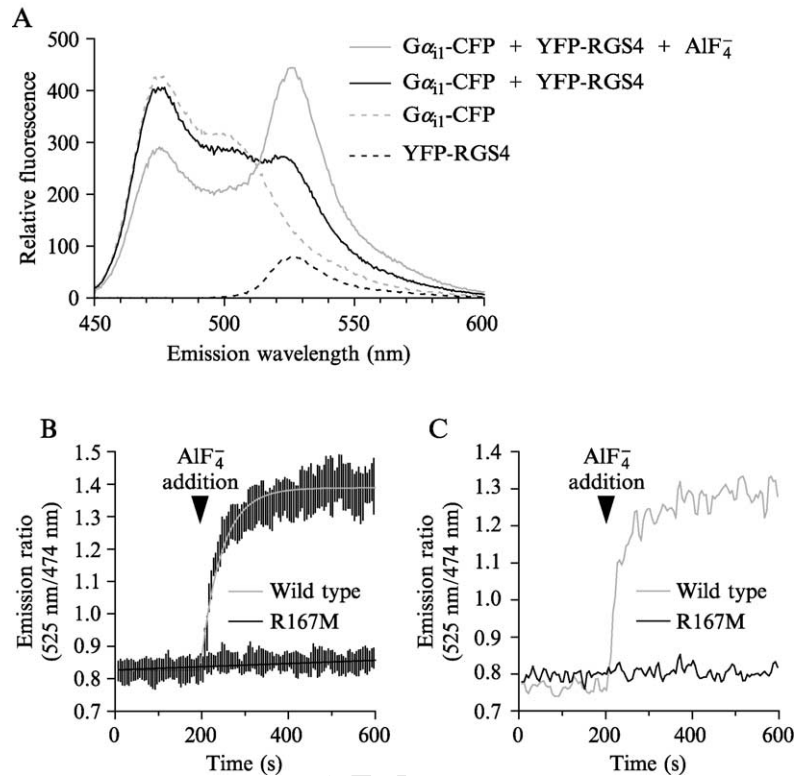


FIG. 2. Aluminum tetrafluoride-dependent FRET between CFP- $G\alpha_{i1}$  and YFP-RGS4 fusion proteins. (A) Sequential emission scans between 450 and 600 nm were conducted using a LS55 spectrofluorimeter in the presence of various combinations of  $G\alpha_{i1}$ -CFP, YFP-RGS4, and/or  $AlF_4^-$ . The excitation wavelength for these emission spectral scans was 433 nm, with excitation and emission slit widths of 2.5 nm. Values are corrected by background subtraction of a buffer control and are normalized to make the peak fluorescence value for the YFP-RGS4 alone condition equal to 100. (B) Real-time measurement of  $AlF_4^-$ -induced FRET between  $G\alpha_{i1}$ -CFP and YFP-RGS4 proteins. Real-time emission ratio (525/474 nm) measurements were made from cuvettes containing 200 nM  $G\alpha_{i1}$ -CFP and 280 nM YFP-RGS4 (wild type) or 280 nM YFP-RGS4 point mutant (R167M) proteins. At 200 s, 20 mM NaF and 30  $\mu$ M  $AlCl_3$  were added to the cuvette to induce  $G\alpha_{i1}$  activation and binding to YFP-RGS4. Triplicate samples were fit to a single-exponential association function. Error bars denote the standard error of the mean. (C) One representative data set from the experiment conducted as described in B.

To measure the spectral dynamics of FRET induced by the binding of  $G\alpha_{i1}$  to RGS4, 40  $\mu$ l of 0.5 M NaF and 1  $\mu$ l of 30 mM  $AlCl_3$  are added to the cuvette (for final concentrations of 20 mM and 30  $\mu$ M, respectively). After a 5-min delay to allow full  $G\alpha_{i1}$  activation ( $t_{1/2} = 33$  s at 20 $^\circ$ ;

assuming single exponential association as illustrated in Fig. 2B), the emission spectrum is read (Fig. 2A). Relative fluorescence values in the  $\text{AlF}_4^-$ -containing sample are corrected for dilution by a factor of 1.041. (*Note:* This corrective step is only necessary in the analysis of spectral data, as emission ratio measurements are essentially independent of protein concentration in the micromolar range; see Fig. 3D.) In comparison to the emission spectrum of  $G\alpha_{i1}$ -CFP and YFP-RGS4 alone, the addition of  $\text{AlF}_4^-$  causes decreased emission at 474 nm (the normal emission peak for CFP) and a concomitant increase in emission at 525 nm (the normal emission peak for YFP) consistent with FRET (Fig. 2A). Thus, by tracking fluorescence emission at these two specific wavelengths (525 nm for YFP; 474 nm for CFP), one can calculate the ratio between the two emission intensities as a sensitive readout of RGS box/ $G\alpha$  association. In this specific example (Fig. 2A), 525/474-nm emission ratio values were calculated as 0.66 (266.2/401.4) for control (no  $\text{AlF}_4^-$ ) and 1.54 (443.3/287.4) in the presence of  $\text{AlF}_4^-$ , producing a 2.5-fold change in ratio by the interaction between  $G\alpha_{i1}$ -CFP and YFP-RGS4.

Real-time measurements of aluminum tetrafluoride-dependent  $G\alpha$ /RGS box interactions have thus far only been described using surface plasmon resonance (Kimple *et al.*, 2001; Popov *et al.*, 1997; see also this volume, Willard and Siderovski, 2004). We have used the  $G\alpha_{i1}$ -CFP and YFP-RGS4 FRET system to evaluate the binding between  $G\alpha_{i1}$  and RGS4 moieties in real time.  $\text{AlF}_4^-$ -dependent  $G\alpha$ /RGS box interaction is measured in the LS55 spectrofluorimeter using 1 ml of buffer F containing 200 nM  $G\alpha_{i1}$ -CFP and 280 nM YFP-RGS4 at 20°. Using the TRUE RATIO mode, the 525/474-nm emission ratio is measured with a data interval of 5 s, encompassing 2s integrations at each wavelength. This is conducted using excitation at 433 nm and excitation and emission slit widths of 2.5 nm. After 200 s, the fluorescence emission ratio should have stabilized, and 41  $\mu\text{l}$  of  $\text{AlF}_4^-$  (40  $\mu\text{l}$  of 0.5 M NaF and 1  $\mu\text{l}$  of 30 mM  $\text{AlCl}_3$ ) is added to the cuvette to induce  $G\alpha$  activation and FRET between the labeled RGS4 and  $G\alpha_{i1}$  proteins. As illustrated in Fig. 2B and C, the addition of  $\text{AlF}_4^-$  increases the FRET emission ratio from 0.8 to 1.4. Increases are rapid and generally plateau after 200–400 s.

As a control to discount nonspecific fluorescence effects as the cause of emission ratio changes, mutant YFP-RGS4 proteins can be employed in this assay. For example, arginine-167 of RGS4 forms a salt bridge with two highly conserved  $G\alpha_{i1}$  residues in the X-ray crystallographic structure of the transition state complex (Tesmer *et al.*, 1997). The R167M mutation inhibits GAP activity and the aluminum tetrafluoride-dependent interaction of RGS4 with  $G\alpha_{i1}$  (Druey and Kehrl, 1997), thus R167M (or one of many other RGS box mutations described in the literature) serves as an

appropriate negative control for these assays. Figures 2B and C illustrate the utility of YFP-RGS4(R167M) as a negative control for this FRET assay. Data from triplicate samples are averaged and fit to a single exponential association curve using Graph Pad Prism, as illustrated in Fig. 2B. The rate of  $\text{AlF}_4^-$ -induced FRET increase is generally comparable to that of the  $\text{AlF}_4^-$ -induced change in intrinsic tryptophan fluorescence that is indicative of  $G\alpha$  activation (Higashijima *et al.*, 1987). The half-time to maximal FRET is calculated, in this case, as 33.3 s. An example of raw data from an individual set of experiments is illustrated in Fig. 2C. These experiments were conducted with just 200–300 nM of protein and thus experimental “noise” is significant. Performing these assays with higher concentrations of protein (i.e., low micromolar amounts) essentially obviates this problem.

#### Development of a High-Throughput FRET Assay for $G\alpha_{i1}$ /RGS4 Interaction

Aluminum tetrafluoride-dependent FRET between  $G\alpha_{i1}$ -CFP and YFP-RGS4 can be measured in a 96-well plate format using a SpectraMax Gemini fluorescence plate reader (Molecular Devices, Sunnyvale, CA). Samples are placed in Costar 96-well, flat-bottom, “special optics” black plates (Corning, Acton, MA). The SpectraMax Gemini is first optimized for CFP/YFP FRET using the SPECTRUM (FLUORESCENCE) function under the INSTRUMENT SETTINGS dialog box in the SOFTmax PRO v3.11 control software (Molecular Devices). This allows for excitation and emission scanning and optimization of cutoff filter settings, as recommended by the manufacturer. For experimental analysis of FRET, the ENDPOINT (FLUORESCENCE) function is used, specifying automatic photomultiplier tube adjustment (PMT AUTO), Costar plates, high sensitivity (30 reads per well), and thorough mixing of samples before readings (AUTOMIX 5 s). For dual ratio emission measurements, wavelength settings are as follows: channel 1, excitation 433 nm, emission 479 nm with a 455-nm cutoff filter and channel 2, excitation 433 nm, emission 529 nm with a 495-nm cutoff filter. FRET is measured using 190  $\mu\text{l}$  buffer F per well containing 200 nM each of  $G\alpha_{i1}$ -CFP and YFP-RGS4 fusion proteins. The SpectraMax Gemini is temperature controlled and plates are equilibrated at 25° for 5 min. An initial reading is then taken to serve as the “preinteraction” measurement. The  $\text{AlF}_4^-$  ion is then formed by the addition of NaF and  $\text{AlCl}_3$  to final concentrations of 20 mM and 30  $\mu\text{M}$  to make up a final, per-well volume of 200  $\mu\text{l}$ . The plate is then incubated for 5 min at 25°, a time period sufficient for complete  $G\alpha_{i1}$  activation and  $G\alpha_{i1}$ /RGS4 complex formation (as determined in Figs. 2B and C). Readings are then made to serve as the “+ $\text{AlF}_4^-$ ”

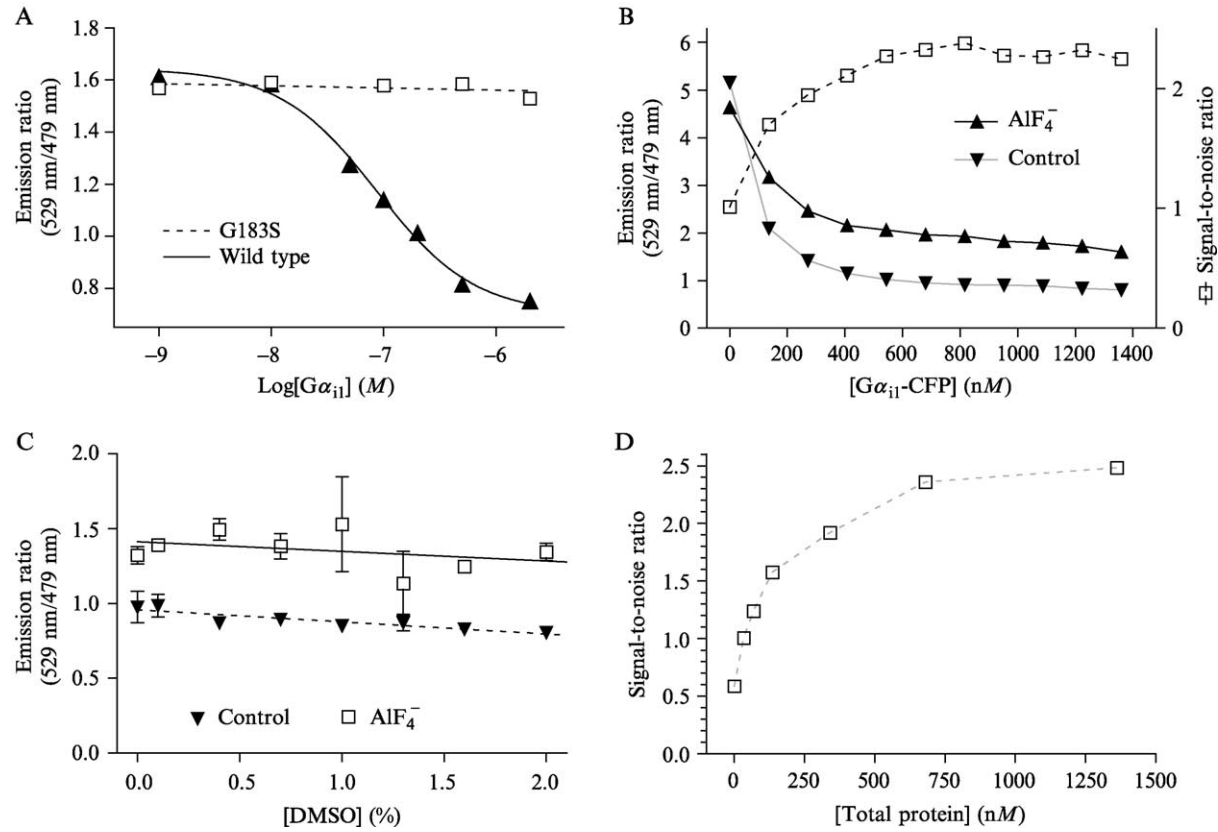


FIG. 3. Optimization of the CFP-Gα<sub>i1</sub>/YFP-RGS4 FRET assay for high-throughput screening of RGS box inhibitors. FRET between CFP-Gα<sub>i1</sub> and YFP-RGS4 was measured using a SpectraMax Gemini 96-well plate fluorescence reader. All emission ratio scans were conducted using an excitation wavelength of 433 nm and dual emission wavelengths of 479 and 529 nm. Samples were

measurement. Initial data analysis (i.e., emission ratio calculation) is accomplished using SOFTmax PRO; subsequent data analysis is done using Graph Pad Prism. Readings from wells containing only buffer with or without  $\text{AlF}_4^-$  are subtracted from sample well readings to account for any buffer effects. We have not observed significant qualitative differences between data analyzed with or without background subtraction (Willard and Siderovski, unpublished observations).

To validate the utility of this assay for the discovery of inhibitors of the  $G_{\alpha_{i1}}$ /RGS4 interaction, we investigated the disruption of the  $G_{\alpha_{i1}}$ -CFP/YFP-RGS4 complex using nonfluorescent  $G_{\alpha_{i1}}$  proteins. Disruption of the interaction between  $G_{\alpha_{i1}}$ -CFP and YFP-RGS4 is measured by first initiating the FRET interaction, as described earlier, with 200 nM  $G_{\alpha_{i1}}$ -CFP, 200 nM YFP-RGS4, 20 mM NaF, and 30  $\mu\text{M}$   $\text{AlCl}_3$ . After a 5-min incubation at 25°, a broad range of concentrations (up to 2  $\mu\text{M}$ ) of His<sub>6</sub>- $G_{\alpha_{i1}}$  or RGS box-insensitive, glycine-183 to serine (G183S) His<sub>6</sub>- $G_{\alpha_{i1}}$  (DiBello *et al.*, 1998; Lan *et al.*, 1998) are added to individual wells. Following a 20-min incubation, FRET is quantitated and data are fit to a dose-response curve with Graph Pad Prism. Disruption of FRET by the wild-type unlabeled  $G_{\alpha_{i1}}$  protein is illustrated in Fig. 3A; this inhibitory effect occurs with an  $\text{IC}_{50}$  of 87 nM. The competitive and specific nature of this disruption is indicated by the failure of His<sub>6</sub>- $G_{\alpha_{i1}}$  G183S to disrupt FRET at a 20-fold molar excess; the glycine-183 to serine point mutation to  $G_{\alpha_{i1}}$  renders the protein unable to interact with RGS proteins (DiBello *et al.*, 1998; Lan *et al.*, 1998).

Further optimization of the  $G_{\alpha_{i1}}$ /RGS4 FRET assay can be achieved by careful titration of the various assay components and reagents. For

---

equilibrated with all reaction components, save for  $\text{AlF}_4^-$ , for 5 min at 25° and then duplicate fluorescence readings were collected. The planar ion  $\text{AlF}_4^-$  was induced by the addition of NaF and  $\text{AlCl}_3$  to final concentrations of 20 mM and 30  $\mu\text{M}$ , respectively. Following a 5-min incubation, duplicate fluorescence readings were collected again. (A) Competitive inhibition of the CFP- $G_{\alpha_{i1}}$ /YFP-RGS4 interaction. This experiment was conducted in the presence of indicated concentrations of nonfluorescent His<sub>6</sub>- $G_{\alpha_{i1}}$  ("wild type") or RGS box-insensitive, point mutant His<sub>6</sub>- $G_{\alpha_{i1}}$  ("G183S"). Data are presented as emission ratio measurements following  $\text{AlF}_4^-$  addition. (B) Titration of CFP- $G_{\alpha_{i1}}$  protein concentration required for effective FRET in the presence of 1400 nM YFP-RGS4. Data on the left ordinate are presented as emission ratio measurements before ("control") and after aluminium tetrafluoride addition (" $\text{AlF}_4^-$ "). The right ordinate scale ("signal-to-noise" ratio) is defined as the ratio of  $\text{AlF}_4^-$ -induced emission ratio to control emission ratio (as described in the text). (C) Tolerance of the FRET assay to dimethyl sulfoxide (DMSO). This experiment was conducted in the presence of indicated concentrations of DMSO. Data are presented as emission ratio measurements before ("control") and after aluminium tetrafluoride addition (" $\text{AlF}_4^-$ "). (D) Dependence of the FRET assay on total fluorescent protein concentration.  $G_{\alpha_{i1}}$ -CFP and YFP-RGS4 proteins were combined in an equimolar ratio and assayed for FRET in a dose-dependent manner up to a total protein concentration of 1.4  $\mu\text{M}$  (1400 nM).

example, preliminary experiments achieved a signal-to-noise ratio of 1.3 (as defined later), whereas optimized assay conditions give a signal-to-noise ratio of over 3.0:

$$\text{signal-to-noise ratio} = \frac{\text{AlF}_4^- (\text{Em}_{529 \text{ nm}}/\text{Em}_{479 \text{ nm}})}{\text{control} (\text{Em}_{529 \text{ nm}}/\text{Em}_{479 \text{ nm}})}$$

Figure 3B illustrates the signal-to-noise ratio using a titration of  $G_{\alpha_{i1}}$ -CFP protein concentration against a constant concentration of 1400 nM YFP-RGS4. The 529/479-nm emission ratios stabilize as the  $G_{\alpha_{i1}}$ -CFP concentration reaches that of YFP-RGS4; similarly, the signal-to-noise increases to above 2. Similar titrations should be performed with all buffer components to maximize the signal-to-noise ratio and facilitate sensitive detection of the  $G_{\alpha_{i1}}$ /RGS4 interaction.

To create a high-throughput screen for small molecule inhibitors of RGS box proteins, it is necessary to validate the tolerance of the assay for the solvents in which the small molecule organic compounds are dissolved. Generally, the solvent of choice is dimethyl sulfoxide (DMSO) (Seethala and Fernandes, 2001). Testing of the DMSO tolerance of the  $G_{\alpha_{i1}}$ /RGS4 FRET assay is conducted essentially as described earlier, but with the addition of DMSO [0–2% (v/v)] and the reading of FRET values before and after  $\text{AlF}_4^-$  addition. Figure 3C illustrates the DMSO sensitivity of this particular assay: the overall fluorescence emission ratio attenuation observed upon DMSO addition does not appear to affect signal-to-noise performance of this assay up to a concentration of 2% (v/v) DMSO. Clearly, for any compound library screening, it will be important to include solvent controls to eliminate false positives.

To examine the detection–response range of the  $G_{\alpha_{i1}}$ /RGS4 FRET assay,  $G_{\alpha_{i1}}$ -CFP and YFP-RGS4 fusion proteins are mixed in an equimolar ratio and a FRET experiment is conducted by titrating the total protein concentration (0–1400 nM) versus the signal-to-noise ratio (as defined earlier). Figure 3D illustrates that a plot of signal-to-noise ratio versus protein concentration is exponential and plateaus above 750 nM total protein. This is an important experimental consideration in assaying for RGS inhibitors, as the larger the molar ratio of inhibitor to RGS box protein that can be achieved, the higher the likelihood of observing inhibitor activity; *in vitro* inhibitors derived from compound libraries will probably have orders of magnitude less affinity to their RGS box targets than the affinity of the  $G_{\alpha}$  subunit/RGS box interaction. The intricacies and numerical considerations of high-throughput screening are well discussed in the literature (e.g., Copeland, 2003). Clearly, it is best to strive for a balance between assay sensitivity and high test compound concentration in such assays.

#### Use of RGS Box Proteins as Biosensors for G-Protein Activation

The FRET assay for the  $G\alpha$ /RGS box interaction can also be utilized to assay the effect of G-protein modulatory peptides on  $G\alpha$  function. We have explored this approach using a synthetic peptide derived from the GoLoco motif of RGS12. GoLoco motifs are guanine nucleotide dissociation inhibitors (GDIs) for the adenylyl cyclase inhibitory class of G-protein  $\alpha$  subunits. GoLoco motif-containing proteins have essential roles in metazoan cell division processes via their regulation of the heterotrimeric G-protein cycle (Kimple *et al.*, 2002a; Willard *et al.*, 2004b). Two of the more rigorously characterized GoLoco motifs are those present in RGS12 and RGS14 (Kimple *et al.*, 2001, 2002b). The GoLoco motifs of RGS12 and RGS14 are potent GDIs for  $G\alpha_i$  but not  $G\alpha_o$  subunits. GoLoco motif peptides from RGS12, RGS14, and AGS3 have been found to stabilize the GDP-bound conformation of  $G\alpha$  (De Vries *et al.*, 2000; Kimple *et al.*, 2001). This activity was measured as refractoriness of GoLoco-liganded  $G\alpha$  subunits to  $AlF_4^-$ -induced activation using intrinsic tryptophan fluorescence assays. The use of intrinsic tryptophan fluorescence can be limited by the weak fluorescence enhancement (60%) achieved upon G-protein activation (Higashijima *et al.*, 1987) and the background fluorescence contributed by any protein cofactor added. We have thus abandoned the intrinsic tryptophan fluorescence assay for this new FRET assay system.

The modulatory effect of the RGS12 GoLoco motif on  $G\alpha$  activation by  $AlF_4^-$  is measured as generally described in the previous section.  $G\alpha_{i1}$ -CFP (200 nM) and YFP-RGS4 (280 nM) are incubated at 25° in a 1-ml cuvette containing 10 mM Tris-HCl, pH 8.0, 200 mM NaCl, 1 mM EDTA, 10 mM  $MgCl_2$ , and 2  $\mu M$  GDP. Test samples contain either a 2- or a 10-fold molar excess of a synthetic peptide encompassing the minimal GoLoco motif of rat RGS12 (RGS12-GoLoco; amino acids 1186–1221) or a vehicle ( $H_2O$ ) control (Kimple *et al.*, 2001). The RGS12-GoLoco peptide is dissolved in  $H_2O$  to a stock concentration of 400  $\mu M$ ; we have also found that purified recombinant GoLoco motif-containing proteins and DMSO-solubilized synthetic peptides are also compatible with this assay (see in this series: Kimple, Willard, and Siderovski, 2004). After incubation for 5 min at 25° to allow complex formation between  $G\alpha$  and RGS12-GoLoco peptide, fluorescence measurements are initiated with excitation at 433 nm (2.5-nm slit width) and dual-emission wavelength detection at 474 nm (2.5-nm slit width) and 525 nm (2.5-nm slit width). (As the salient data obtained in this assay are kinetic, only one sample is measured using the LS55 spectrofluorimeter. However, for end point FRET studies, and those assays where kinetics are not imperative, multiple

sample measurements can be conducted using a 96-well plate reader, as described earlier.)

After 150 s, the fluorescence emission ratio should have stabilized, and 41  $\mu\text{l}$  of  $\text{AlF}_4^-$  (40  $\mu\text{l}$  of 0.5 M NaF and 1  $\mu\text{l}$  of 30 mM  $\text{AlCl}_3$ ) is added to

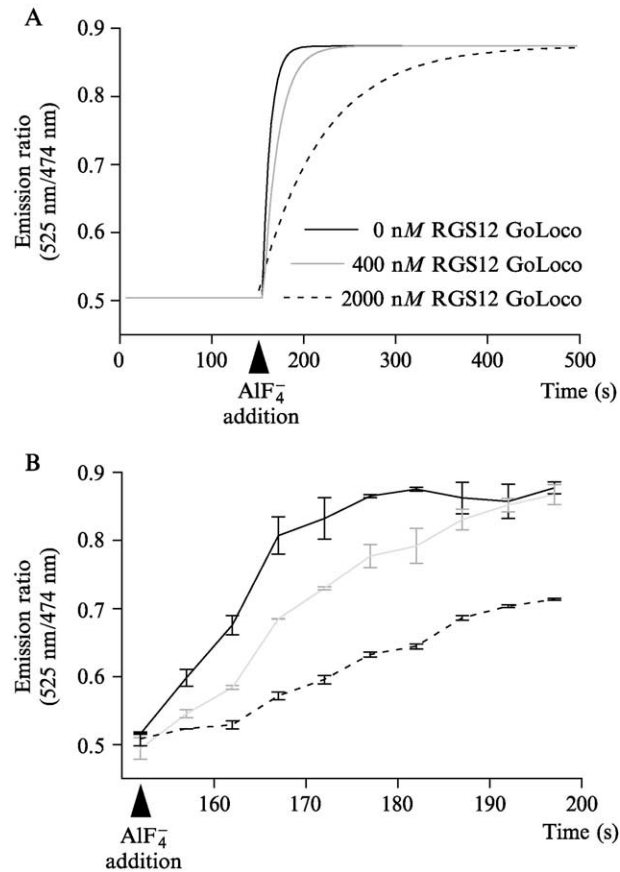


FIG. 4. Analysis of GoLoco motif peptide inhibition of  $G\alpha_{i1}$  activation by the use of FRET between  $G\alpha_{i1}$ -CFP and YFP-RGS4. (A) FRET between 200 nM  $G\alpha_{i1}$ -CFP and 280 nM YFP-RGS4 was measured, in real time, as a ratio of emission intensity at 525 nm to an emission intensity at 474 nm. FRET pair samples contained RGS12 GoLoco peptide (400 or 2000 nM) or a vehicle control. At 150 s, planar ion  $\text{AlF}_4^-$  was created by the addition of NaF and  $\text{AlCl}_3$  to final concentrations of 20 mM and 30  $\mu\text{M}$ , respectively. Duplicate experiments were averaged and fit to a single exponential association function using Graph Pad Prism. (B) Raw data from the experiment conducted in A are presented over the period immediately following the addition of  $\text{AlF}_4^-$ , illustrating the dramatic attenuation of the G-protein activation rate in the presence of RGS12 GoLoco peptide. Data points are the mean  $\pm$  SEM of duplicate experiments.

the cuvette to induce  $G\alpha$  activation and FRET between  $G\alpha_{i1}$ -CFP and YFP-RGS4. In general, the addition of excess volume to reactions does not need to be accounted for with corrective calculations, as the emission ratio measurement for FRET does not depend on total protein concentration; rather, the relative protein concentration is the important factor (Figs. 3B and D). Figure 4A illustrates attenuation of  $G\alpha_{i1}$  activation by the RGS12-GoLoco peptide, present at suprastoichiometric concentrations over the input amount of  $G\alpha_{i1}$ -CFP (200 nM). Figure 4A represents data from duplicate samples that were subsequently fit to a single exponential association model using Graph Pad Prism. This analysis yielded initial  $G\alpha$  activation rates for samples containing 0 nM ( $1.2 \times 10^{-1} \pm 7.3 \times 10^{-3} \text{ s}^{-1}$ ), 400 nM ( $6.2 \times 10^{-2} \pm 1.6 \times 10^{-3} \text{ s}^{-1}$ ), and 2000 nM ( $1.4 \times 10^{-2} \pm 2.7 \times 10^{-4} \text{ s}^{-1}$ ) RGS12-GoLoco peptide. Thus, a 2-fold molar excess of RGS12-GoLoco peptide (400 nM) to  $G\alpha_{i1}$ -CFP (200 nM) gave a 2-fold decrease in the  $G\alpha_{i1}$  activation rate, whereas a 10-fold molar excess of RGS12-GoLoco peptide (2000 nM) gave a 12-fold decrease in activation rate. These findings suggest that this assay can accurately measure the attenuation of  $\text{AlF}_4^-$ -mediated  $G\alpha$  activation by GoLoco motif peptides and, presumably, other  $G\alpha$ -binding peptides/proteins. Raw data from the experiment in Fig. 4A over the time period immediately following  $\text{AlF}_4^-$  addition are presented in Fig. 4B to illustrate the dramatic attenuation of the G-protein activation rate in the presence of the RGS12-GoLoco peptide that can be observed in real time.

#### Concluding Remarks

We have described protocols for the accurate measurement of the interaction between  $G\alpha_{i1}$  and RGS4 using FRET. This assay is effective in measuring the activities of both mutant  $G\alpha_{i1}$  (i.e., G183S) and mutant RGS4 (i.e., R167M) proteins and should be amenable to any  $G\alpha$ /RGS box pair that can be purified as soluble recombinant proteins. There remains the potential for this assay to be modified and utilized *in vivo* to detect receptor-mediated heterotrimer activation and we are currently pursuing this approach. Furthermore, we have investigated the use of the  $G\alpha_{i1}$ -CFP and YFP-RGS4 protein pair to create a microtiter plate-formatted high-throughput assay for RGS-box/ $G\alpha$  interaction inhibitors. Finally, we have described a novel assay for detecting the modulatory effects of other  $G\alpha$  interactors (e.g., GoLoco motif peptides) on G-protein activation by aluminum tetrafluoride—an assay that is uniquely able to resolve the subtle kinetics of this activation process.

## Acknowledgments

We thank Dr. Catherine Berlot for the provision of ECFP and EYFP cDNAs (Weis Centre for Research, Danville, PA). FSW is an American Heart Association Postdoctoral Fellow. RJK is supported by a predoctoral fellowship from the National Institutes of Mental Health (F30 MH64319). This work was funded by NIH Grants R01 GM062338 and P01 GM065533. Thanks to Dr. Benjamin Yerxa and the rest of Inspire Pharmaceuticals Inc. for support in the initial phase of this project. DPS is a recipient of the Burroughs Wellcome Fund New Investigator Award in the Basic Pharmacological Sciences and a Year 2000 Scholar of the EJLB Foundation.

## References

- Berman, D. M., Wilkie, T. M., and Gilman, A. G. (1996a). GAIP and RGS4 are GTPase activating proteins for the Gi subfamily of G protein alpha subunits. *Cell* **86**, 445–452.
- Berman, D. M., Kozasa, T., and Gilman, A. G. (1996). The GTPase-activating protein RGS4 stabilizes the transition state for nucleotide hydrolysis. *J. Biol. Chem.* **271**, 27209–27212.
- Copeland, R. A. (2003). Mechanistic considerations in high throughput screening. *Anal. Biochem.* **320**, 1–12.
- De Vries, L., Fischer, T., Tronchere, H., Brothers, G. M., Strockbine, B., Siderovski, D. P., and Farquhar, M. G. (2000). Activator of G protein signaling 3 is a guanine dissociation inhibitor for G-alpha i subunits. *Proc. Natl. Acad. Sci. USA* **97**, 14364–14369.
- DiBello, P. R., Garrison, T. R., Apanovitch, D. M., Hoffman, G., Shuey, D. J., Mason, K., Cockett, M. I., and Dohlman, H. G. (1998). Selective uncoupling of RGS action by a single point mutation in the G protein alpha-subunit. *J. Biol. Chem.* **273**, 5780–5784.
- dos Remedios, C. G., and Moens, P. D. (1995). Fluorescence resonance energy transfer spectroscopy is a reliable “ruler” for measuring structural changes in proteins. Dispelling the problem of the unknown orientation factor. *J. Struct. Biol.* **115**, 175–185.
- Druey, K. M., and Kehrl, J. H. (1997). Inhibition of regulator of G protein signaling function by two mutant RGS4 proteins. *Proc. Natl. Acad. Sci. USA* **94**, 12851–12856.
- Gilman, A. G. (1987). G proteins: Transducers of receptor-generated signals. *Annu. Rev. Biochem.* **56**, 615–649.
- Heikal, A. A., Hess, S. T., Baird, G. S., Tsien, R. Y., and Webb, W. W. (2000). Molecular spectroscopy and dynamics of intrinsically fluorescent proteins: Coral red (dsRed) and yellow (Citrine). *Proc. Natl. Acad. Sci. USA* **97**, 11996–12001.
- Higashijima, T., Ferguson, K. M., Sternweis, P. C., Ross, E. M., Smigel, M. D., and Gilman, A. G. (1987). The effect of activating ligands on the intrinsic fluorescence of guanine nucleotide binding regulatory proteins. *J. Biol. Chem.* **262**, 752–756.
- Kimple, R. J., Willard, F. S., and Siderovski, D. P. (2002a). The GoLoco Motif: Heralding a new tango between G protein signaling and cell division. *Mol. Intervent.* **2**, 88–100.
- Kimple, R. J., Kimple, M. E., Betts, L., Sondek, J., and Siderovski, D. P. (2002b). Structural determinants for GoLoco induced inhibition of nucleotide release by G-alpha subunits. *Nature* **416**, 878–881.
- Kimple, R. J., De Vries, L., Tronchere, H., Behe, C. I., Morris, R. A., Gist Farquhar, M., and Siderovski, D. P. (2001). RGS12 and RGS14 GoLoco motifs are G-alpha(i) interaction sites with guanine nucleotide dissociation inhibitor activity. *J. Biol. Chem.* **276**, 29275–29281.
- Kimple, R. J., Jones, M. B., Shutes, A., Yerxa, B. R., Siderovski, D. P., and Willard, F. S. (2003). Established and emerging fluorescence based assays for G-protein function: Heterotrimeric G-protein-alpha subunits and regulator of G protein signaling (RGS) proteins. *Comb. Chem. High Throughput Screen.* **6**, 399–407.

- Kimple, R. J., Willard, F. S., and Siderovski, D. P. (2004). Purification and *in vitro* functional analyses of R6S12 and RGS14 GoLoco-motif peptides. *Methods Enzymol.* **390**(26), 419–436.
- Lakowicz, J. R. (1999). “Principles of Fluorescence Spectroscopy.” Kluwer Academic/Plenum, New York.
- Lan, K. L., Sarvazyan, N. A., Taussig, R., Mackenzie, R. G., DiBello, P. R., Dohlman, H. G., and Neubig, R. R. (1998). A point mutation in Galphao and Galphail blocks interaction with regulator of G protein signaling proteins. *J. Biol. Chem.* **273**, 12794–12797.
- Lan, K. L., Zhong, H., Nanamori, M., and Neubig, R. R. (2000). Rapid kinetics of regulator of G-protein signaling (RGS)-mediated Galphai and Galphao deactivation. Galpha specificity of RGS4 and RGS7. *J. Biol. Chem.* **275**, 33497–33503.
- Miyawaki, A., and Tsien, R. Y. (2000). Monitoring protein conformations and interactions by fluorescence resonance energy transfer between mutants of green fluorescent protein. *Methods Enzymol.* **327**, 472–500.
- Mukhopadhyay, S., and Ross, E. M. (1999). Rapid GTP binding and hydrolysis by G(q) promoted by receptor and GTPase-activating proteins. *Proc. Natl. Acad. Sci. USA* **96**, 9539–9544.
- Neubig, R. R., and Siderovski, D. P. (2002). Regulators of G-protein signalling as new central nervous system drug targets. *Nature Rev. Drug Discov.* **1**, 187–197.
- Pierce, K. L., Premont, R. T., and Lefkowitz, R. J. (2002). Seven-transmembrane receptors. *Nature Rev. Mol. Cell. Biol.* **3**, 639–650.
- Popov, S., Yu, K., Kozasa, T., and Wilkie, T. M. (1997). The regulators of G protein signaling (RGS) domains of RGS4, RGS10, and GAIP retain GTPase activating protein activity *in vitro*. *Proc. Natl. Acad. Sci. USA* **94**, 7216–7220.
- Prasher, D. C., Eckenrode, V. K., Ward, W. W., Prendergast, F. G., and Cormier, M. J. (1992). Primary structure of the *Aequorea victoria* green-fluorescent protein. *Gene* **111**, 229–233.
- Seethala, R., and Fernandes, P. B. (2001). “Handbook of Drug Screening.” Dekker, New York.
- Tesmer, J. J., Berman, D. M., Gilman, A. G., and Sprang, S. R. (1997). Structure of RGS4 bound to AIF4-activated G(i alpha1): Stabilization of the transition state for GTP hydrolysis. *Cell* **89**, 251–261.
- Willard, F. S., and Siderovski, D. P. (2004). *Methods Enzymol.* **389**(19), (this volume).
- Willard, F. S., Kimple, A. J., Kimple, R. J., and Siderovski, D. P. (2004a). “Toward small molecule inhibitors of RGS proteins: Development of computational and *in vitro* fluorescence-based approaches.” *FASEB J.* **18**(4), A 219 (abstract 165.4).
- Willard, F. S., Kimple, R. J., and Siderovski, D. P. (2004b). Return of the GDI: The GoLoco Motif in cell division. *Annu. Rev. Biochem.* **73**, 925–951.